



Characterization of well logs using K-mean cluster analysis

Amjad Ali¹ · Chen Sheng-Chang¹

Received: 13 October 2019 / Accepted: 25 April 2020 / Published online: 6 May 2020
© The Author(s) 2020

Abstract

The identification process of different lithologies, hydrocarbons, and water-saturated zones in oil and gas industries involves petrophysical studies that are carried out by geoscientists using different software packages. This study aims to propose a method by integrating mean cluster analysis and well logs to identify dominant lithologies, pore fluids, and fluids contact. For this purpose, initially, K-mean cluster analysis is applied to density log and P-wave velocity data of three wells in order to group them into different clusters. Based on centroids of each cluster, different lithologies have been identified. The density log equation has been utilized to compute the porosity of each cluster, and the mean of each density log cluster is used as matrix density. Next, sonic log equation has been inverted to compute the fluid velocity and the mean of each P-wave velocity cluster is used as matrix velocity. For the fluid density, sonic and density log equations are jointly inverted to compute the fluid velocity of each cluster. The fluid bulk modulus and acoustic impedance are computed using fluid density and velocity. Based on the results of K-mean cluster analysis, different lithologies (shale, sandstone, and limestone) have been recognized successfully. In well-1, hydrocarbon and water-saturated zones are successfully identified and fluids contact has been established in the zone of interest. However, well-2 and well-3 did not show any indications of the presence of hydrocarbon in the respective zones.

Keywords K-mean cluster analysis · Density log · P-wave velocity · Fluid velocity · Fluid bulk modulus · Acoustic impedance

Introduction

In the oil and gas exploration industry, generally, petrophysicists interpret well logs on the basis of their previous professional experience to identify hydrocarbon, water saturation zones, and fluids contact. The interpretation of well logs changes from person to person, and this mainly depends on the experience and knowledge of a geoscientist while the reserves estimation is a fundamental part of exploration activity. The characterization of pore fluids and fluids contact in a reservoir is very important for volumetric computation of reserves estimation in a hydrocarbon reservoir (Chombart 1960).

Over the period of time, numerous techniques have been developed for reservoir characterization. For example, Gutierrez et al. (2000) used a rock physics model to identify pore fluids from the sonic log and Mukerji et al. (2001) integrated rock physics and seismic data through geostatistics in order to reduce the uncertainty of seismic reservoir characterization while Mark Sams (2001) used the geostatistical inversion for lithological and impedance modeling for reservoir characterization. Afterward, Galikeev and Davis (2003) merged 4D seismic attributes and geostatistics for thin carbonate reservoir characterization while González et al. (2006) integrated rock physics and seismic inversion using multipoint geostatistics for reservoir characterization. Later on, Jiang and Yang (2012) incorporated stochastic inversion and petrophysical properties for a better understanding of subsurface rock properties. Furthermore, MacAllister et al. (2014) used rock physics with AVO analysis to identify stratigraphic reservoir and Nicholls et al. (2014) utilized 3D and 4D rock physics parameters to get a better picture of the reservoir and enhance the production. Moreover, Jing et al. (2015)

✉ Amjad Ali
aali@zju.edu.cn

Chen Sheng-Chang
chenshengc@zju.edu.cn

¹ School of Earth Sciences, Zhejiang University,
Hangzhou City, Zhejiang Province, China

did the quantitative studies and integrated the rock physics with seismic to identify hydrocarbon-saturated zone. During the same period of time, Yang et al. (2015) combined the elastic properties with AVO for quantitative studies to identify potential hydrocarbon reservoir and Bredeesen et al. (2015) incorporated rock physics with AVO to identify the source and reservoir rocks while Wang et al. (2016) used three new rock physics parameters approximation from AVO for deep reservoir studies and Xiuwei and Zhu (2016) used stochastic impedance inversion using the well and seismic data with the control sedimentary facies. On the other side, Huidong et al. (2016) used the multi-point geostatistical model for reservoir characterization of a sand body and Jie et al. (2016) utilized AVO and seismic tuning for the identification of thin layer hydrocarbon reservoir. Recently, Gomes de Mello e Silva and Beneduzi (2017) applied an empirical method to sonic log to identify pore fluid in a siliciclastic reservoir and Ali and Al-Shuhail (2018) did the joint inversion of P-wave velocity and impedance to identify fluids contact. Zhou et al. (2017) used the asymptotic equation for fluid identification in a carbonate reservoir.

In the present world, artificial intelligence and computer machines are playing a very important role. Due to their wide range of applications, researchers are turning towards the combination of artificial intelligence and computer machines. They are seeking their applications in every field of science. For example, Lin and Salisch (1994) presented a mathematical model by combining principle component and cluster analysis along with Bayes discriminant analysis to determine different lithologies, porosity, and permeability. Euzen et al. (2010) integrated cluster analysis and electrofacies in order to identify an unconventional hydrocarbon prospect in Upper Mannville incised valley. Dudley et al. (2016) combined the borehole data and cluster analysis with real-time microseismic data to characterize an unconventional reservoir. Cluster analysis is an unsupervised machine learning algorithm of clustering/grouping a large dataset into significant subgroups so that the data points in same class have same characteristics and different from another subgroup. It was first introduced by Queen (1966). It has a number of applications in various fields, for example data mining (Fayyad et al. 1996), compression of data, and quantization of vector (Gersho and Gray 2012). Generally, K-mean cluster analysis is used for continuous datasets (Fukunaga 2013; Duda et al. 1973). The purpose of clustering is to discover important patterns in large datasets (Wagstaff 2012). K-mean cluster analysis is easy and simple to understand, and it is fast and robust to cluster large dataset. In this study, in order to minimize the human error during the interpretation of well logs and to get the better reliable results, we are going to integrate K-mean cluster analysis and well logs to identify dominant lithologies and zone of interest in the well logs. It

can be a helpful tool to interpret large well logs datasets and it can reduce human error in order to get better and reliable results.

Methodology

In this study, we have incorporated three wells logs for the computation purpose. The physical structure of the methodology can be seen in Fig. 1. K-mean cluster analysis is a well-known clustering algorithm because of its easy implementation and efficiency (Nazeer and Sabes-tian 2009). K-mean clustering is an unsupervised learning algorithm, and the main aim of K-mean clustering is to partition n number of observations into K number of clusters. For the numerical dataset, the center of each cluster is represented by the mean/centroid. In each cluster, every observation belongs to the nearest mean. Mathematically, K-mean cluster analysis can be written as (Wang et al. 2012);

$$J = \sum_{j=1}^k \sum_{i=1}^n x_i^{(j)} - C_j^2 \quad (1)$$

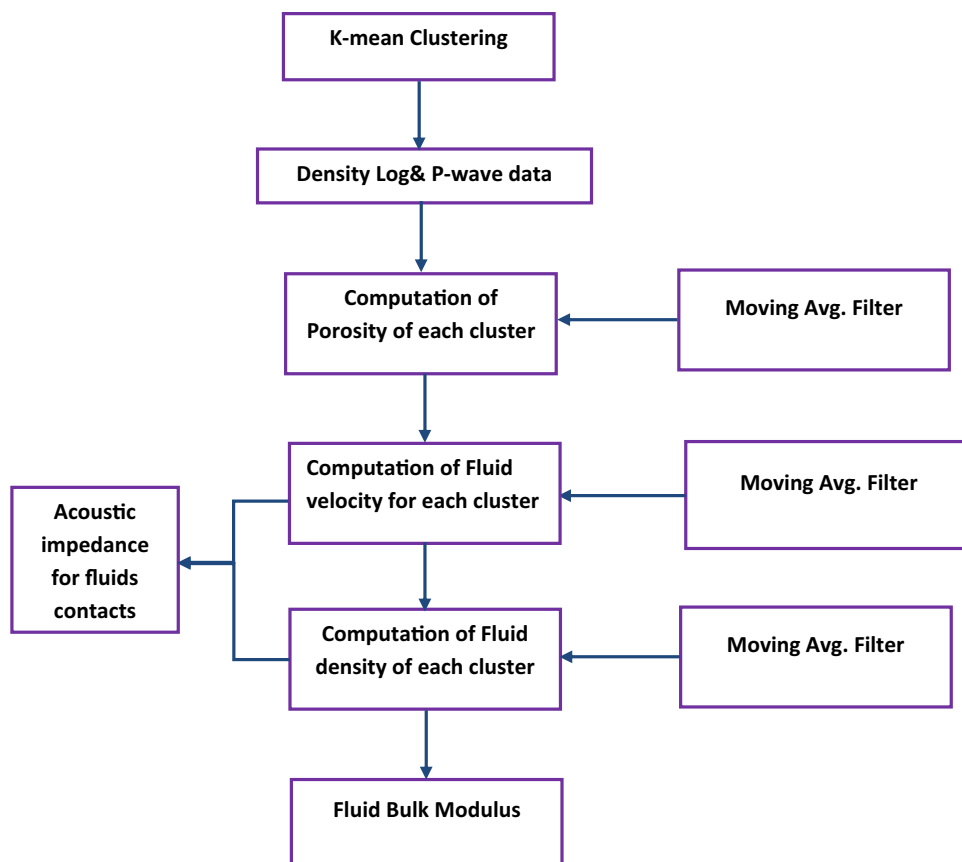
here in Eq. 1, J is an objective function, K is number of clusters, n is the number of observations, $x_i^{(j)}$ is the observation, and C_j is centroid for cluster j . K-mean cluster analysis works in the following way;

1. First, we need to select the number of clusters (K) randomly.
2. Based on the number of clusters, the K-mean cluster will divide the data points into subsets and it will allocate the centroids to each subset or cluster.
3. Then we will redefine the number of clusters (K) and K-mean will compute the clusters again and assign the data points to their nearest centroids.
4. The second and third step will be iterating until the arithmetic means/centroids do not change any more.

At first stage, we need to select an arbitrarily number of clusters for the given dataset and then compute the distance between each data points and cluster and allocate it to nearest cluster. Now update the number of clusters and its averages. Then redefine the number of cluster and compute the new averages and assign the data points to the new cluster based on their closest cluster. Repeat this process, until there is no change in centroids.

K-mean clustering is a very efficient and robust method, but we need to predefine the number of clusters (K). There is no optimal number of clusters, and the best approach is to compute multiple clusters and compare the results of each cluster analysis and choose the best one.

Fig. 1 Workflow chart of the proposed methodology



In this study, initially, K-mean clustering is applied to the density log and P-wave velocity data of three wells to group them into different clusters and to get the mean of each cluster. The mean value of each cluster is given in Table 1. After K-mean clustering of each well, the density log equation is used to compute the porosity of each density log cluster, as (Alger et al. 1963):

$$\varnothing = \frac{\rho_m - \rho_b}{\rho_m - \rho_f} \tag{2}$$

where \varnothing is porosity in fraction, ρ_m is matrix density in g/cm^3 and is the mean of each density log cluster, as given in Table 1, and ρ_b is bulk density value from density log in g/cm^3 . ρ_f is the fluid density value, and here it is considered as $1.1 g/cm^3$ value of brine water.

After this, the moving average filter is used to remove any outliers from the porosity values and to make the porosity of each cluster smooth and acceptable.

Then P-wave velocity is computed from the sonic log as:

$$V_p = \left(\frac{10^6}{3.28} * DT \right) \tag{3}$$

In Eq. 3, V_p is P-wave velocity in m/s and DT are sonic log values.

Here the sonic log equation has been used to compute the fluid velocity (Tixier et al. 1959);

$$\frac{1}{V_p} = \frac{\varnothing}{V_f} + \frac{(1 - \varnothing)}{V_m} \tag{4}$$

here V_p is P-wave velocity computed from the sonic log in m/s, \varnothing is porosity in fraction, V_f is fluid velocity in m/s, and V_m is matrix velocity in m/s.

Sonic log equation (Eq. 4) is inverted to compute the fluid velocity of each cluster of P-wave velocity data, as:

$$V_f = \frac{V_p * (\varnothing - \varnothing^2) - V_m * \varnothing}{(1 - \varnothing)} \tag{5}$$

here in Eq. 5, V_f and V_p are fluid velocity and P-wave velocity in m/s, respectively. V_m is matrix velocity, and it is the mean of each cluster of P-wave velocity data, as given in Table 1. \varnothing

Table 1 Mean values of each cluster

S/no	Cluster	Mean value (ρ_m) (g/cm ³)	Mean value (V_m) (m/s)	Lithology
<i>Well-1</i>				
1	Cluster-1	2.013	1671	Shale Sandstone Limestone Sandstone
2	Cluster-2	2.066	1768	
3	Cluster-3	2.067	2062	
4	Cluster-4	2.15	2369	
5	Cluster-5	2.153	2582	
6	Cluster-6	2.46	2781	
7	Cluster-7	2.699	3604	
8	Cluster-8	2.487	3029	
9	Cluster-9	2.513	3397	
<i>Well-2</i>				
1	Cluster-1	2.129	2190	Shale
2	Cluster-2	2.286	2541	Sandstone
3	Cluster-3	2.295	2920	
4	Cluster-4	2.389	3175	
5	Cluster-5	2.53	3456	
6	Cluster-6	2.556	3641	
7	Cluster-7	2.614	3391	
8	Cluster-8	2.621	3302	
9	Cluster-9	2.644	3710	
<i>Well-3</i>				
1	Cluster-1	2.12	1910	Shale
2	Cluster-2	2.169	2480	Sandstone
3	Cluster-3	2.511	3297	
4	Cluster-4	2.568	4863	
5	Cluster-5	2.452	3519	
6	Cluster-6	2.482	3402	

is porosity in fraction and fluid velocity is computed for each cluster, and then, moving average filter is used to remove any outliers.

For the computation of fluid density, the density log Eq. 2 and sonic log Eq. 4 are inverted as:

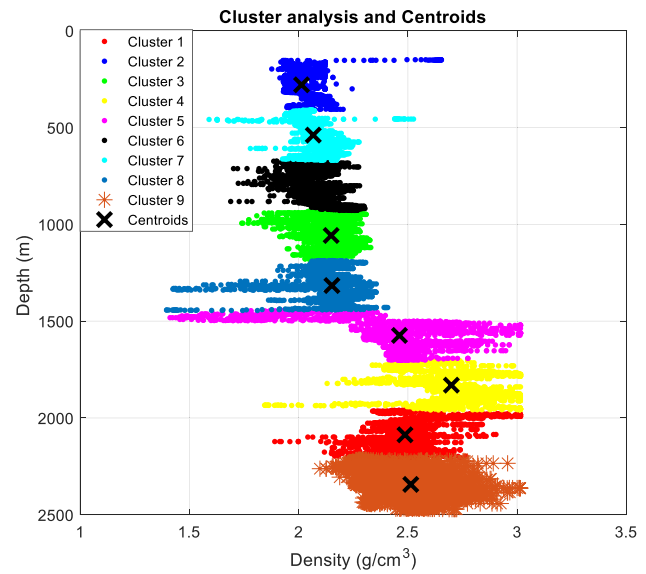
$$\rho_f = \rho_m - \frac{(\rho_m - \rho_b) * V_p (V_m - V_f)}{V_f (V_m - V_p)} \quad (6)$$

The fluid density is computed for each cluster, and then, moving average filter is used to remove any outliers. The fluid bulk modulus is computed as:

$$K_f = (V_f^2 * \rho_f * 1000) \quad (7)$$

here in Eq. 6, K_f is fluid bulk modulus in Pascal.

Generally, acoustic impedance is the product of the density and velocity of rocks. In this the study to confirm the fluids contact, we used the fluid density and fluid velocity in order to establish and confirm the fluids contact, as:

**Fig. 2** Well-1 cluster analysis of density log

$$AI = V_f * \rho_f * 1000 \quad (8)$$

here in Eq. 7, AI is acoustic impedance in kg s/m².

Results

In this study, three different well logs data have been used for the computation purpose. Initially, K-mean clustering is adopted for the cluster analysis of density log and P-wave velocity data in order to group these two datasets into different clusters and to get the mean of each cluster. The mean of each cluster of density log and P-wave velocity data is used as matrix density and matrix velocity for further computation, respectively. The porosity, fluid velocity, fluid bulk modulus, and AI are computed in order to identify main lithologies, a potential hydrocarbon reservoir, pore fluids, and fluids contact.

Cluster analysis and porosity computation

K-mean cluster analysis clustered the density log and P-wave velocity data of well-1 and well-2 into 9 and well-3 into 6 clusters, respectively, as shown in Figs. 2, 3, 4, 5, 6, and 7. For the porosity computation, the density log equation (Eq. 2) has been used to compute porosity for each cluster of density logs. Figures 8, 9, and 10 are correlation matrix plots between porosity and density of each well, respectively. For each cluster, K-mean cluster analysis gave us the centroid. Based on the centroid of each cluster, lithological discrimination has been done; centroids along with their respective lithologies are tabulated in Table 1. The standard published

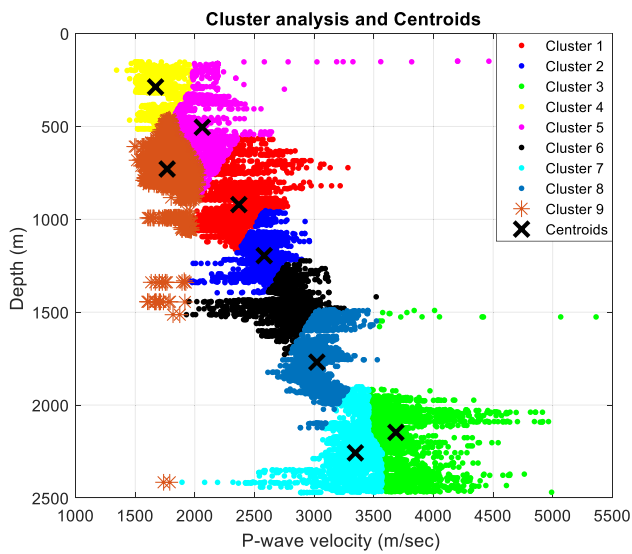


Fig. 3 Well-1 cluster analysis of P-wave Velocity

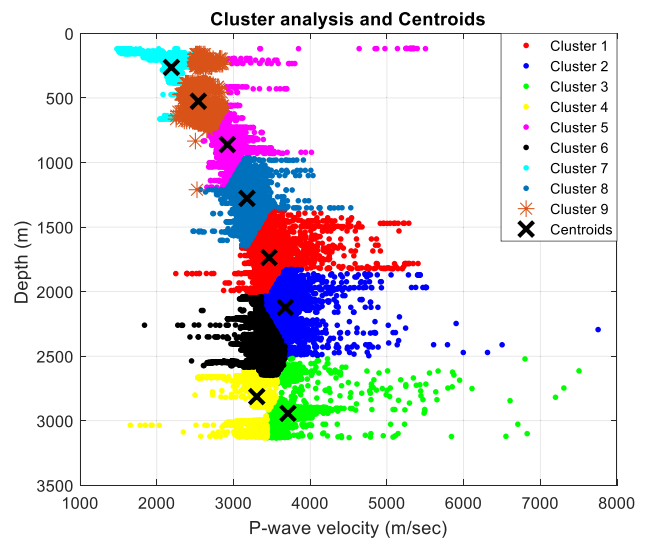


Fig. 5 Well-2 cluster analysis of P-wave velocity

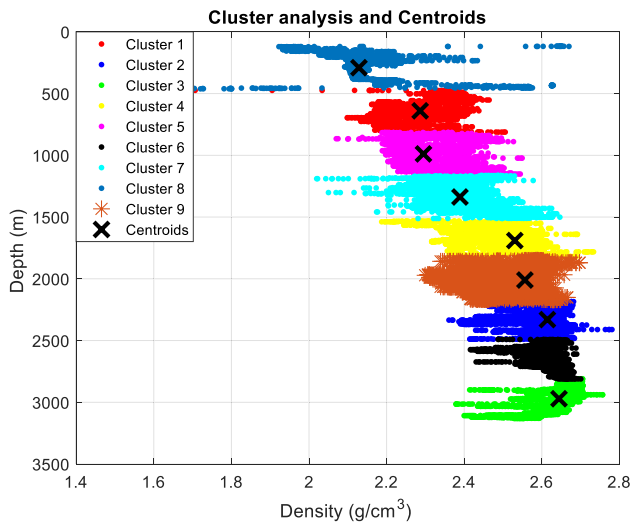


Fig. 4 Well-2 cluster analysis of density log

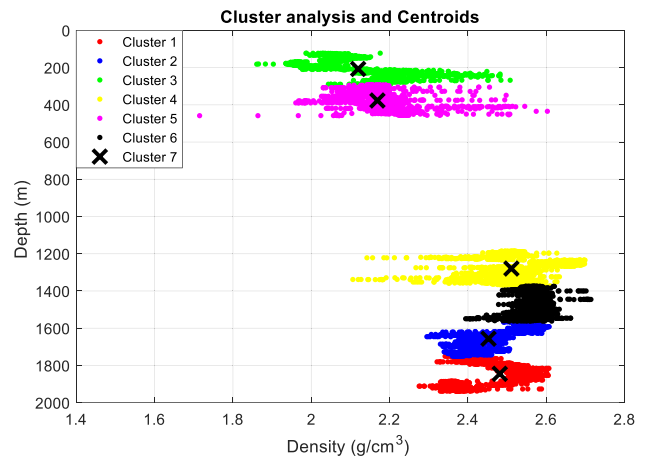


Fig. 6 Well-3 cluster analysis of density log

value of matrix density of quartz is 2.65 g/cm^3 (for sandstone) and calcite is 2.71 g/cm^3 , and it uses for limestone. Matrix density actually represents the mineral density of rock, and mostly rocks are heterogeneous. So instead of using the published values for matrix density and matrix velocity, the centroid of each cluster is used as matrix density (ρ_m) and matrix velocity (V_m) for further computation, respectively. For all the three wells, the values of ρ_m and V_m of each cluster are given in Table 1.

For well-1, based on the mean of each cluster, four main lithologies are distinguished. From surface to 1500 m, the mean of the first 5 clusters are $\leq 2.2 \text{ g/cm}^3$ so it is categorized as shale; then from 1500 to 1750 m, the mean of sixth cluster is 2.5 g/cm^3 and it is categorized as sandstone;

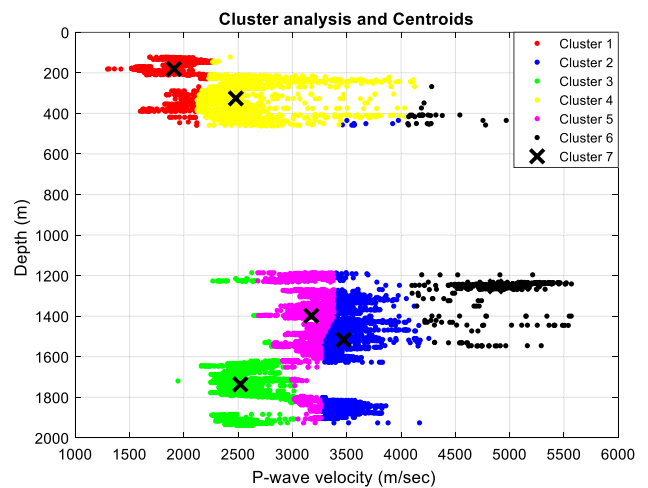
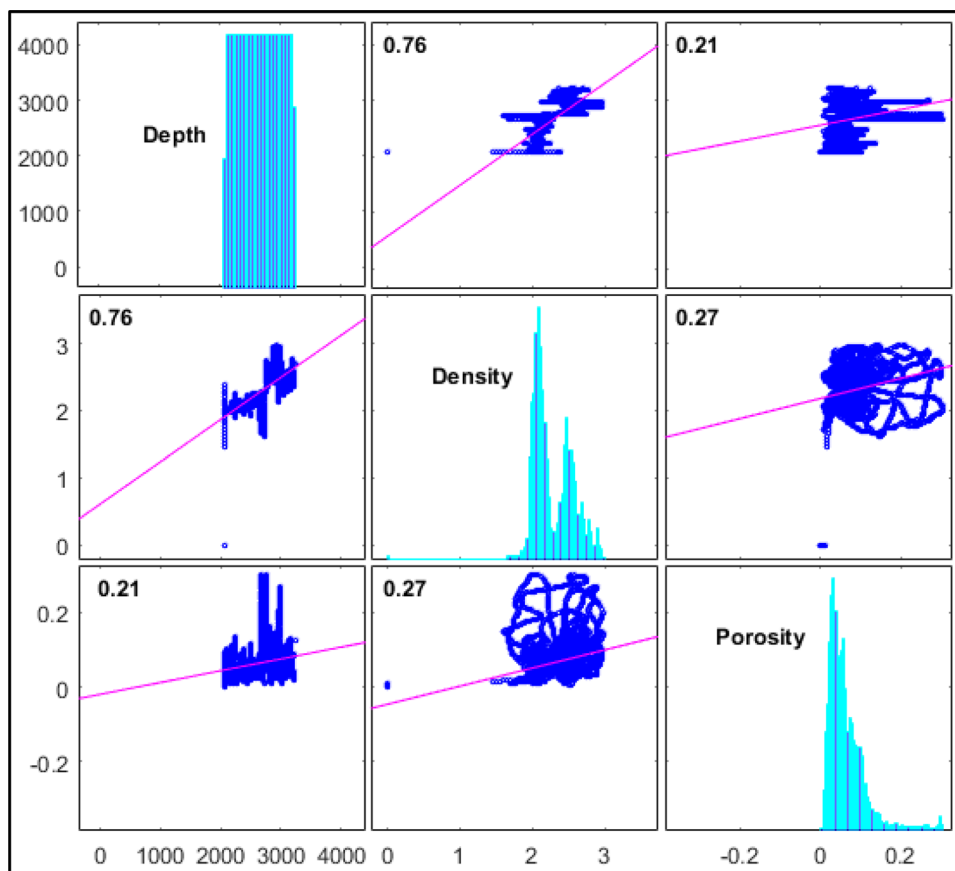


Fig. 7 Well-3 cluster analysis of P-wave velocity

Fig. 8 Correlation matrix of well-1 among depth, density, and porosity with diagonal histogram and correlation coefficient



next, from 1750 to 2000 m, the mean of seventh cluster is 2.7 g/cm^3 and it is categorized as limestone; and last, from 2000 to 2500 m, the mean of eighth and ninth clusters is $\leq 2.5 \text{ g/cm}^3$ and they are categorized as sandstone, as shown in Fig. 8. So, there are three main zones of interest based on lithology distribution which are starting from 1500 to 2500 m. Porosity in the zones of interest is ranging from < 5 to 30%, as shown in Fig. 8.

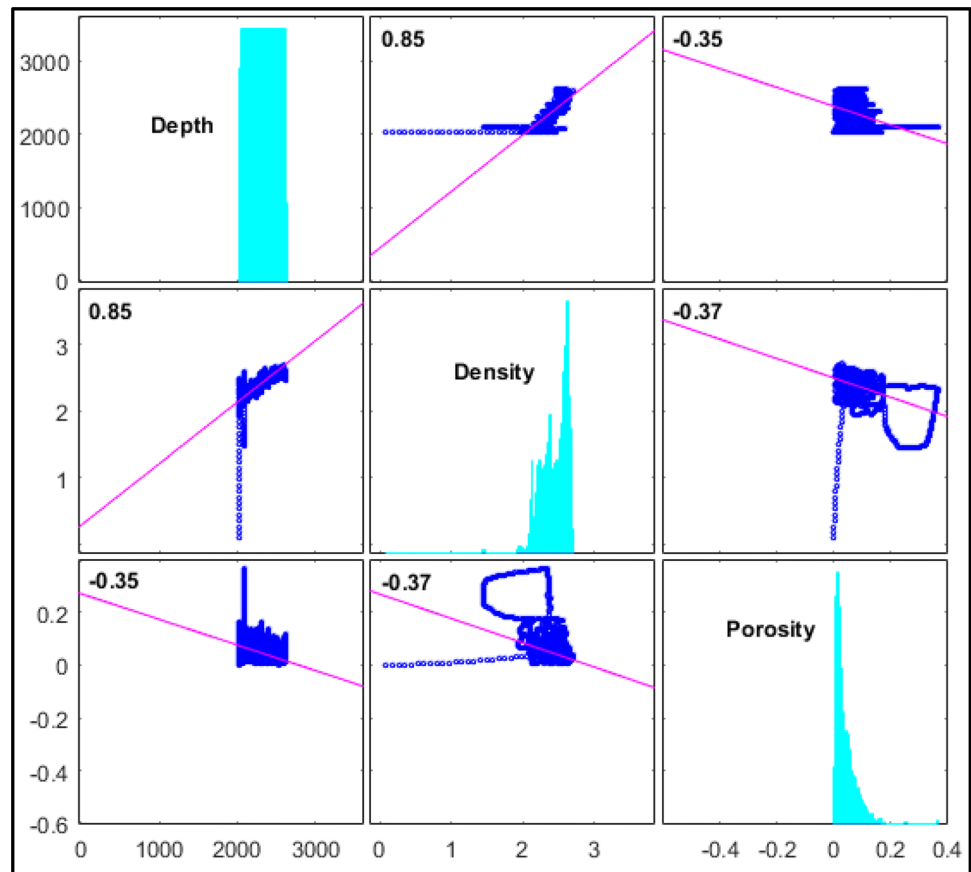
For well-2, based on the mean of each cluster, two main lithologies are identified. From surface to 1500 m, the mean of first 4 clusters is $\leq 2.2 \text{ g/cm}^3$ so it is categorized as shale, while the mean of remaining clusters has $\geq 2.5 \text{ g/cm}^3$; therefore, they are categorized as sandstone dominant lithology. In the sandstone dominant part, the porosity is ranging from < 1 to 15%, as shown in Fig. 9.

For well-3, based on the mean of each cluster, two main lithologies are identified. From surface to 450 m, the mean of the first two clusters is $< 2.2 \text{ g/cm}^3$ so it is categorized as shale, while the mean of remaining clusters has 2.5 g/cm^3 ; therefore, they are categorized as sandstone dominant lithology. In the sandstone dominant part, the porosity is ranging from < 1 to 25%, as shown in Fig. 10. In Table 2, for all three wells, porosities with their corresponding depths and lithologies are tabulated.

Pore fluids and fluids contact identification

For the fluid velocity computation, Eq. 5 has been used to compute the fluid velocity for each cluster of all three wells. Initially, K-mean cluster analysis is applied to P-wave velocity data to cluster it into 9 and 6 clusters, respectively, and to get the mean of each cluster, as shown in Figs. 5, 6, and 7. Instead of using the published values of matrix velocity from the literature for the computation, the mean of each cluster of P-wave velocity data is used as matrix velocity. Figure 11 is the cross-plots of fluid velocity, bulk modulus, and acoustic impedance of well-1. Based on data distribution, the green color (fluid velocity) is ranging from 1250 to 1800 m/s and it is identified as brine water-saturated zones while the data distribution of red color (fluid velocity) is ranging from 0 to 800 m/s and it is identified as hydrocarbon-saturated zones. The cross-plots of fluid bulk modulus and acoustic impedance also endorse the results of fluid velocity, as shown in Fig. 11. Based on fluid velocity, bulk modulus, acoustic impedance, the hydrocarbon-saturated zones suggest that it is live oil. Using fluid bulk modulus and acoustic impedance, two fluid contacts are marked at two different depths, first at 1500 m and second at 1950 m.

Fig. 9 Correlation matrix of well-2 among depth, density, and porosity with diagonal histogram and correlation coefficient



The results of fluid velocity, bulk modulus, and the acoustic impedance of well-2 and well-3 did not give us any prominent indication about the presence of hydrocarbon reservoir in the sandstone dominant part, as shown in Figs. 12 and 13. This shows that the well-2 and well-3 were not successful exploratory wells. The fluid velocity range in these two wells exhibits that there are some traces of hydrocarbon present.

Conclusion

Well logs interpretation is an important part of exploration activity in order to identify different lithologies, zone of interest, and volumetric computation of reserves estimation. In exploration industry, these objectives are mainly achieved through the experience of a geoscientist, which varies from person to person. Human error always exists during the interpretation process. The main objective of

this study is to overcome this human error through integration of K-mean cluster analysis with well logs to identify main lithologies, the zone of interest, pore fluids, and fluids contact. In the absence of prior knowledge of the subsurface lithologies and formations, all the objectives have been successfully achieved through this study. At the first stage, K-mean clustering is applied to density log and P-wave velocity data to make the clusters. Based on the centroids of each cluster, the dominant lithologies are identified. The porosity and fluids velocity of each cluster are computed. Finally, fluid bulk modulus and AI are computed for each cluster to confirm the existence of pore fluids and fluids contact. This study shows that:

- K-mean cluster analysis is an easy and robust algorithm to implement.
- K-mean cluster analysis is a good tool to identify the main subsurface lithologies.

Fig. 10 Well correlation matrix of well-3 among depth, density, and porosity with diagonal histogram and correlation coefficient

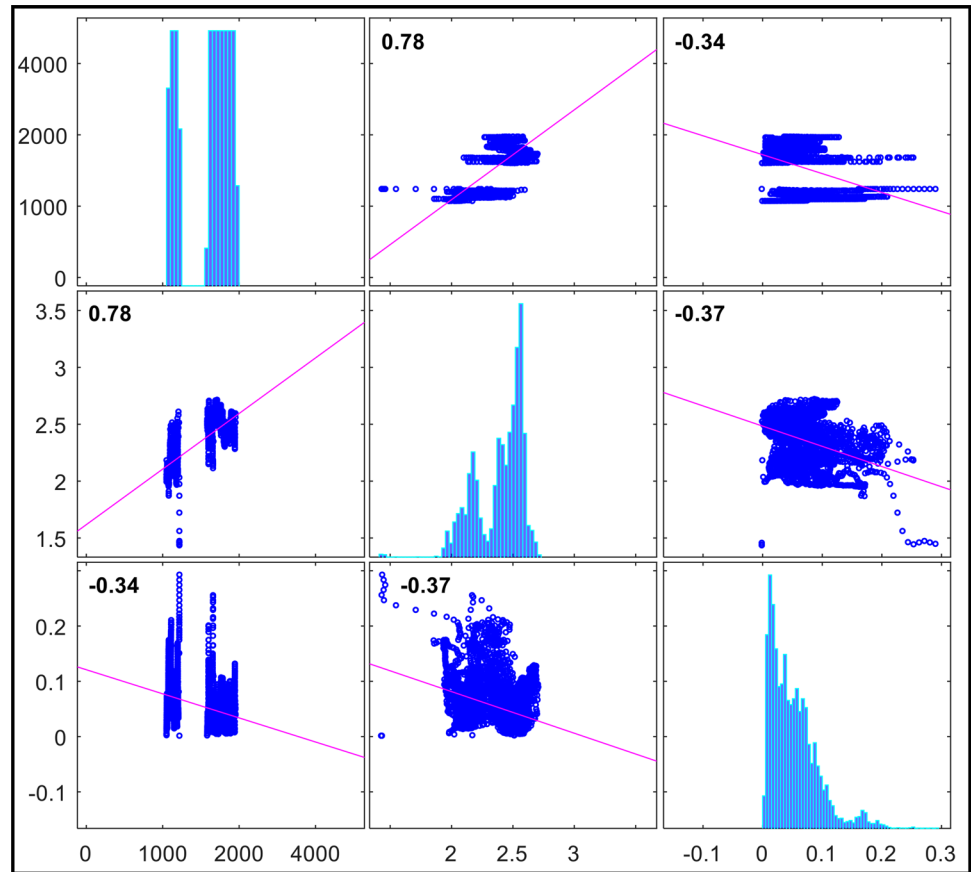


Table 2 Porosity with their corresponding lithologies and depths in each well

S/no	Depth range (m)	Lithology	Porosity range
<i>Well-1</i>			
1	0–1500	Shale	0–30%
2	1500–1750	Sandstone	1–30%
3	1750–2000	Limestone	1–27%
4	2000–2500	Sandstone	1–13%
<i>Well-2</i>			
1	0–1500	Shale	0–35%
2	1500–3130	Sandstone	1–16%
<i>Well-3</i>			
1	0–425	Shale	0–21%
2	1200–1940	Sandstone	1–25%

- Based on the centroids of cluster analysis, we can identify the zone of interest in well logs.
- K-mean cluster analysis is a good tool to minimize human error during the interpretation of well logs.
- The standard published value of matrix density actually represents the mineral density of rock, and mostly rocks are heterogeneous. So instead of using published data for matrix density and velocity, we can use the mean of each cluster as matrix density and velocity.
- Inversion of fluid velocity, fluid bulk, and acoustic impedance is good tools, and if they are integrated with K-mean cluster analysis, these parameters can be helpful to identify the pore fluids and fluids contact.

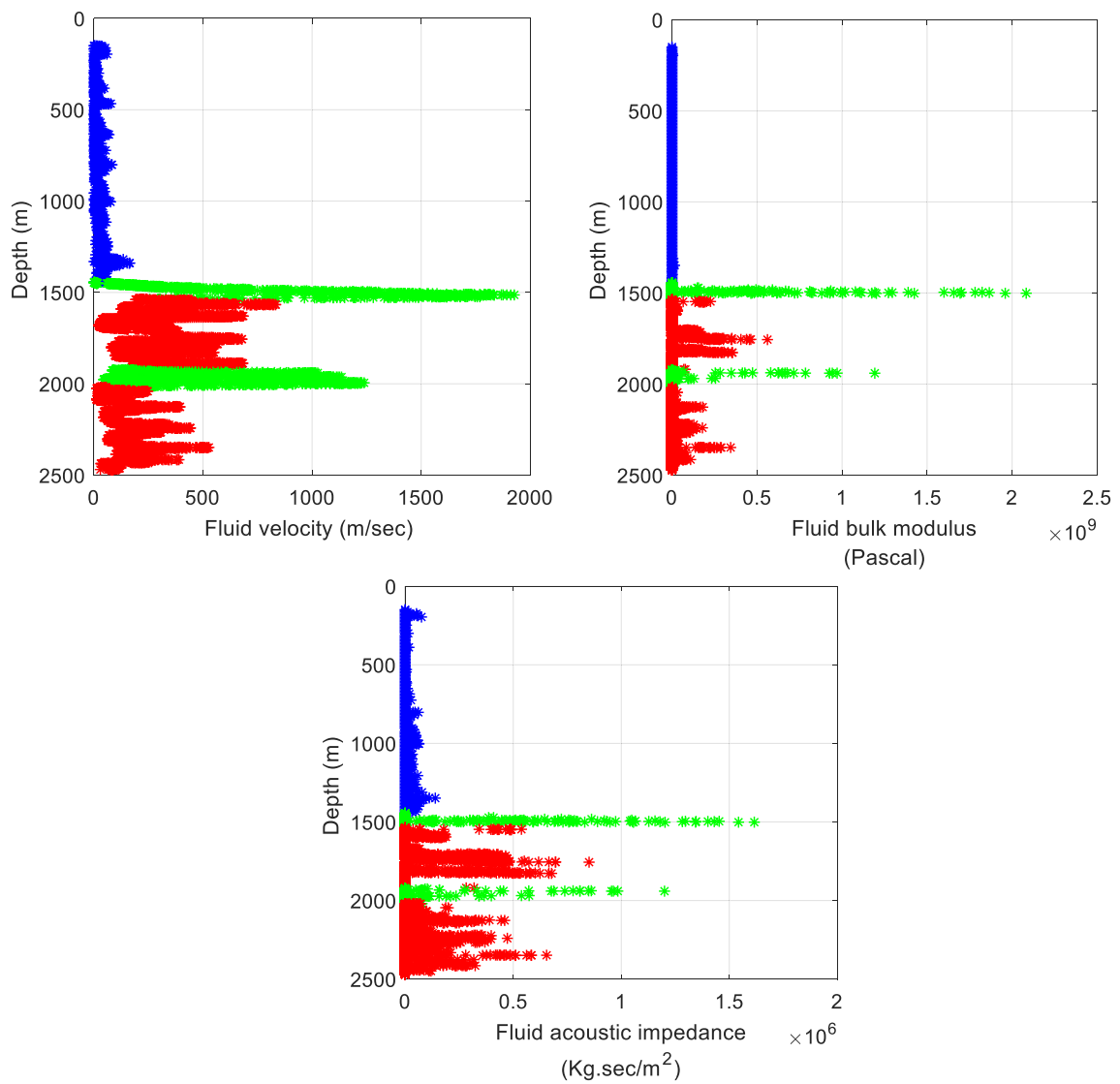


Fig. 11 Fluid velocity, bulk modulus, and acoustic impedance well-1

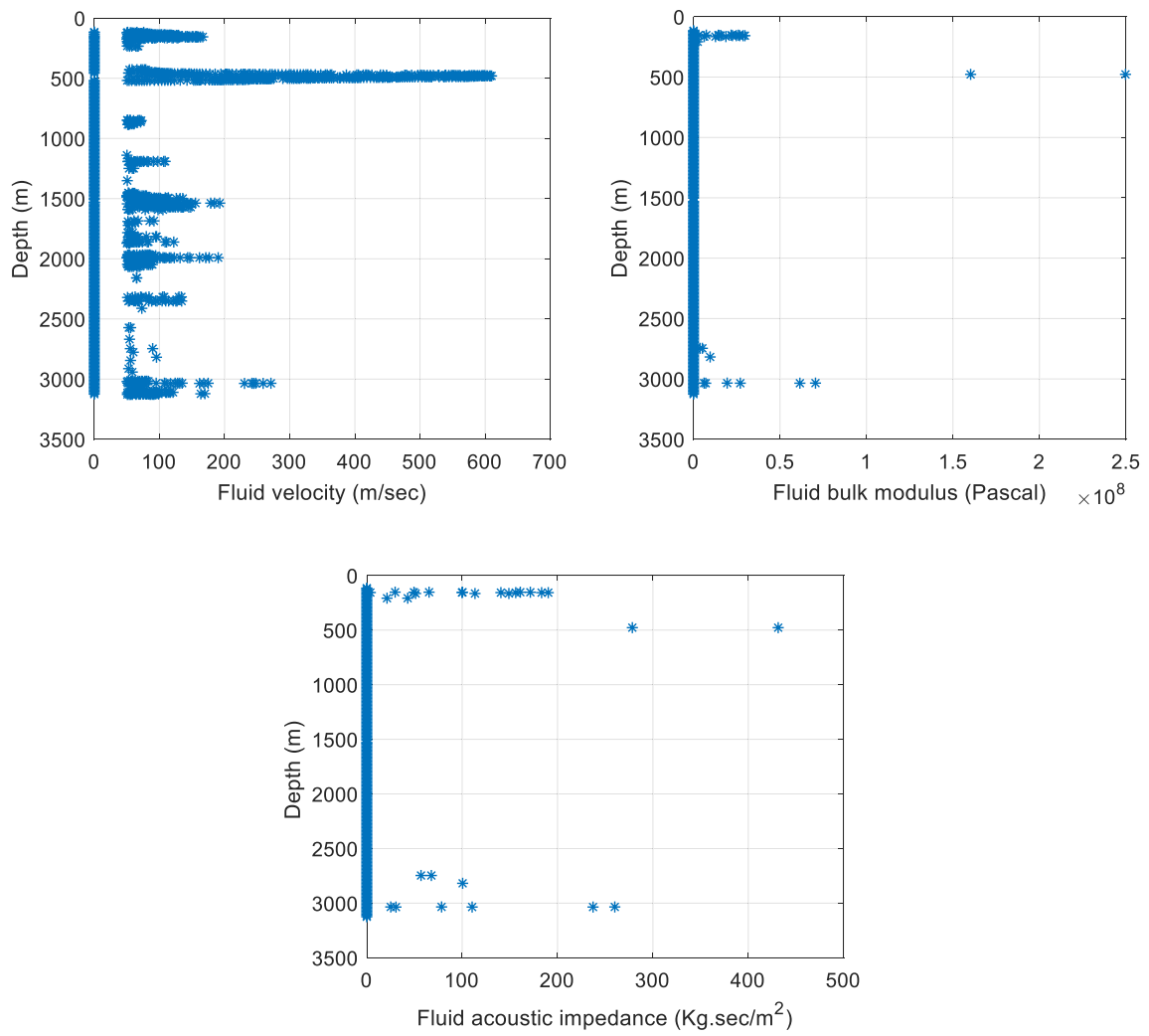


Fig. 12 Fluid velocity, bulk modulus, and acoustic impedance of well-2

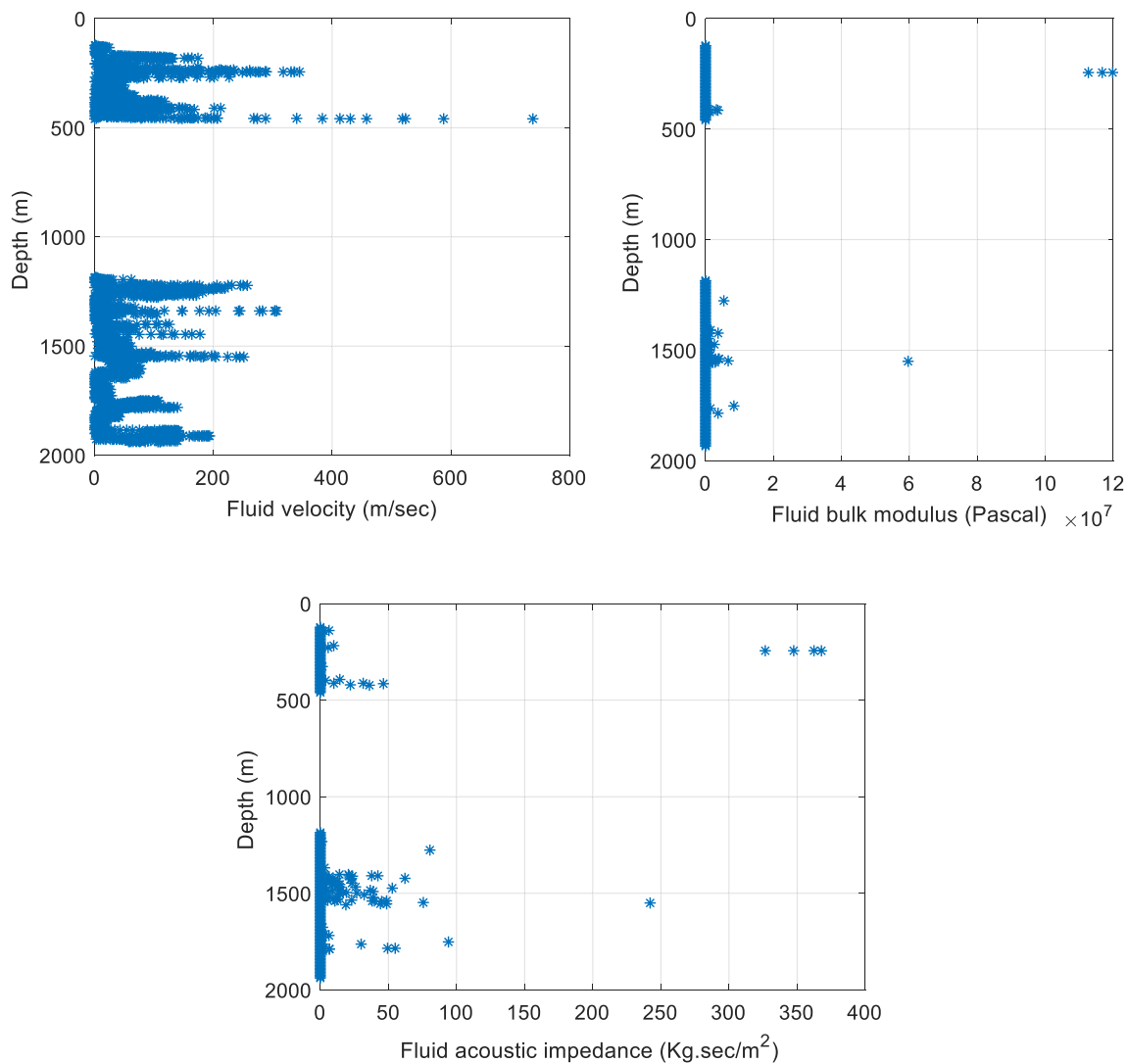


Fig. 13 Fluid velocity, bulk modulus, and acoustic impedance of well-3

Open Access This article is licensed under a Creative Commons Attribution 4.0 International License, which permits use, sharing, adaptation, distribution and reproduction in any medium or format, as long as you give appropriate credit to the original author(s) and the source, provide a link to the Creative Commons licence, and indicate if changes were made. The images or other third party material in this article are included in the article's Creative Commons licence, unless indicated otherwise in a credit line to the material. If material is not included in the article's Creative Commons licence and your intended use is not permitted by statutory regulation or exceeds the permitted use, you will need to obtain permission directly from the copyright holder. To view a copy of this licence, visit <http://creativecommons.org/licenses/by/4.0/>.

References

- Alger RP, Raymer LL Jr (1963) Formation density log applications in liquid-filled holes. *J Pet Technol* 15(03):321–332. <https://doi.org/10.2118/435-PA>
- Ali A, Al-Shuhail AA (2018) Characterizing fluid contacts by joint inversion of seismic P-wave impedance and velocity. *J Pet Explor Prod Technol* 8(1):117–130. <https://doi.org/10.1007/s13202-017-0394-3>
- Bredesen K, Jensen EH, Johansen TA, Avseth P (2015) Seismic reservoir and source-rock analysis using inverse rock-physics modeling: a Norwegian Sea demonstration. *Lead Edge* 34(11):1350–1355. <https://doi.org/10.1190/tle34111350.1>

- Chombart LG (1960) Well logs in carbonate reservoirs. *Geophysics* 25(4):779–853. <https://doi.org/10.1190/1.1438763>
- Duda RO, Hart PE, Stork DG (1973) *Pattern classification and scene analysis*. Wiley, New York
- Dudley C, Davis T, Bratton T, Andersen (2016) Integrating horizontal borehole imagery and cluster analysis with microseismic data for niobrara reservoir characterization, Wattenberg Field, Colorado, USA Unconventional Resources Technology Conference, San Antonio, Texas, 1–3 August 2016 (pp. 2368–2381): Society of Exploration Geophysicists, American Association of Petroleum Geologists, Society of Petroleum Engineers
- Euzen T, Delamaide E, Feuchtwanger T, Kingsmith KD (2010) Well log cluster analysis: an innovative tool for unconventional exploration. Paper presented at the Canadian Unconventional Resources and International Petroleum Conference, Calgary, Alberta, Canada. <https://doi.org/10.2118/137822-MS>
- Fayyad UM, Piatetsky-Shapiro G, Smyth P, Uthurusamy R (1996) *Advances in knowledge discovery and data mining*, vol 21. AAAI press Menlo Park
- Fukunaga K (2013) *Introduction to statistical pattern recognition*. Elsevier, Amsterdam
- Galikeev T, Davis TD (2003) Reservoir modeling of a thin carbonate reservoir using geostatistics and 4-D seismic attributes, Weyburn field, Saskatchewan, Canada SEG technical program expanded abstracts, pp 1354–1357
- Gersho A, Gray RM (2012) *Vector quantization and signal compression*, vol 159. Springer, Berlin
- González EF, Mavko G, Mukerji T (2006) Rock physics and multiple-point geostatistics for seismic inversion. SEG technical program expanded abstracts, pp 2047–2051
- Gutierrez MA, Dvorkin J, Nur A (2000) In-situ hydrocarbon identification and reservoir monitoring using sonic logs, La Cira-Infantas oil field (Colombia). SEG technical program expanded abstracts, pp 1727–1730
- Huidong Y, Baoquan S, Yong H, Liuying H (2016) Numerical reservoir characterization techniques based on multiple point geostatistics. In: SPG/SEG 2016 international geophysical conference, Beijing, China, 20–22, pp 22–25
- Jiang W-l, Yang K (2012) Petrophysical-properties stochastic inversion combining geostatistics and statistical rock-physics: applications to seismic data near ODP1144. SEG technical program expanded abstracts, pp 1–5
- Jie W, Zhen Z, Yun L Impact study on AVO fluid identification for thin interbed reservoir. In: SPG/SEG 2016 international geophysical conference, Beijing, China, 20–22 April 2016, pp 122–125
- Jing B, Ren J, Qin X (2015) Inversion of reservoir properties: Quantitative hydrocarbon seismic identification in tight carbonate reservoirs. SEG technical program expanded abstracts, pp 2693–2697
- Lin JL, Salisch HA (1994) Determination from well logs of porosity and permeability in a heterogeneous reservoir. Paper presented at the SPE Asia Pacific oil and gas conference, Melbourne, Australia. <https://doi.org/10.2118/28792-MS>
- MacAllister K, Daley T, Bacon M, Tamfu S, Nguema P Integration of rock physics and seismic interpretation—an overlooked West African stratigraphic hydrocarbon play. SEG technical program expanded abstracts, pp 1380–1384
- Mukerji T, Avseth P, Mavko G, Takahashi I, González EF (2001) Statistical rock physics: combining rock physics, information theory, and geostatistics to reduce uncertainty in seismic reservoir characterization. *Lead Edge* 20(3):313–319. <https://doi.org/10.1190/1.1438938>
- Nazeer KA, Sebastian M (2009) Improving the accuracy and efficiency of the k-means clustering algorithm. Paper presented at the proceedings of the world congress on engineering
- Nicholls M, Marler S, Maguire D (2014) Integrating 3D and 4D rock physics inversion data into better understanding of field and reservoir behavior to mitigate production decline. SEG technical program expanded abstracts, pp 2798–2802
- Queen M (1966) Some methods for classification and analysis of multivariate observations (Methods for classification and analysis of multivariate observations)
- Sams M (2001) Geostatistical lithology modeling. ASEG extended abstracts: 15th geophysical conference, pp 1–4
- Silva FGM, Beneduzi CF (2017) Using sonic log for fluid identification in siliciclastic reservoirs. In: 15th international congress of the Brazilian geophysical society & EXPOGEEF, Rio de Janeiro, Brazil, 31 July-3 August 2017, pp 872–877
- Tixier MP, Alger RP, Doh CA (1959) Sonic logging, pp 9. Society of Petroleum Engineers
- Wagstaff K (2012) Machine learning that matters. arXiv preprint [arXiv:1206.4656](https://arxiv.org/abs/1206.4656)
- Wang Q, Wang C, Feng Z-Y, Ye J-F (2012) Review of K-means clustering algorithm. *Electron Des Eng* 20(7):21–24
- Wang H, Yin X, Danping C, Zhou Q, Sun W (2016) Three term AVO approximation of $\frac{\partial \log K}{\partial \log \rho}$ and prestack seismic inversion for deep reservoir. SEG technical program expanded abstracts, pp 3693–3697
- Xiuwei Y, Zhu P (2016) A fast stochastic impedance inversion under control of sedimentary facies based on geostatistics and gradual deformation method. SEG technical program expanded abstracts, pp 3746–3750
- Yang J, Chang X, Yang Z (2015) The solution of non-gas bright-spot and non-bright-spot gas identification: Elastic prediction. SEG technical program expanded abstracts, pp 595–599
- Zhou Y, Li Y, Zhao W, Wang M, Hu D, Jiang N (2017) Fluid identification of carbonate reservoir by using asymptotic equation based on two-phase media. SEG 2017 workshop: carbonate reservoir E&P Workshop, Chengdu, China, 22–24 October 2017, pp 116–119

Publisher's Note Springer Nature remains neutral with regard to jurisdictional claims in published maps and institutional affiliations.